



OPEN

Removal of toxic lead from aqueous solution using a low-cost adsorbent

Mohammad Hadi Dehghani^{1,2}, Sahar Afsari Sardari³, Mojtaba Afsharnia⁴, Mehdi Qasemi⁵ & Mahmoud Shams⁶✉

Valorization of waste materials and byproducts as adsorbents is a sustainable approach for water treatment systems. Pottery Granules (PG) without any chemical and thermal modification were used as a low-cost, abundant, and environmentally benign adsorbent against Pb(II), the toxic metal in drinking water. The porous structure and complex mineral composition of PG made it an efficient adsorbent material for Pb(II). The effect of key physicochemical factors was investigated to determine the significance of contact time, PG dose, pH, solution temperature, and coexisting ions, on the process. Pb(II) removal increased by PG dose in the range of 5–15 g/L, and agitation time from 5 to 60 min. Increasing Pb(II) concentration led to a drop in Pb(II) removal, however, adsorption capacity increased significantly as concentration elevated. Pb(II) removal also increased significantly from ~45% to ~97% by pH from 2 to 12. A ~20% improvement in Pb(II) adsorption after rising the solution temperature by 30°C, indicated the endothermic nature of the process. The sorption was described to be a favorable process in which Pb(II) was adsorbed in a multilayer onto the heterogeneous PG surface. The q_{max} of 9.47 mg/g obtained by the Langmuir model was superior among many reported low-cost adsorbents. The Pb(II) adsorption was described well by the Pseudo-first-order kinetic model. Na^+ , Mg^{2+} , Ca^{2+} , Cd^{2+} , and Zn^{2+} showed a negligible effect on Pb(II) adsorption. However, the presence of Mn^{2+} and Fe^{2+} significantly hindered the process efficacy. In conclusion, the use of waste material such as PG against Pb(II) is a viable option from the economic and effectiveness points of view.

Environmental pollution with heavy metals could impose significant impacts on human health and the environment due to the non-biodegradable and accumulative nature^{1–3}. Contamination of water resources by emerging contaminants such as heavy metals by industrial discharges is a serious challenge, especially in developing countries^{4–7}. Mining, smelting, fossil fuels combustion, solid waste incineration, manufacturing batteries, paints, electronic, ceramics, and glass industries are among the anthropogenic sources of heavy metals. Natural phenomena such as forest fires, volcanos, mineral weathering, and erosion, also are responsible for the occurrence of heavy metals^{8–10}.

Pb(II) is a non-essential, toxic, and enzyme inhibitor heavy metal with an MCLG of zero¹¹. Studies endorsed the intake of Pb(II) as an etiological factor for serious damage to the central nervous system, reproductive system, liver, and kidney^{12–15}. However Pb(II) could penetrate the body by different routes, the ingestion through drinking water was known as the main pathway for Pb(II) intake¹⁶. Even in developed countries, there is a growing concern for lead exposure by the presence of Pb(II) at levels exceeding the drinking water standard^{17,18}. Two general strategies exist to abate the negative consequences of this toxic contaminant in drinking water, corrosion control, and removal. USEPA suggested corrosion control as a “treatment technology” to prevent leaching noxious Pb(II) from the old water plumbing¹⁹. Another option, Pb(II) removal from contaminated streams, was studied extensively in recent years.

¹Department of Environmental Health Engineering, School of Public Health, Tehran University of Medical Sciences, Tehran, Iran. ²Institute for Environmental Research, Center for Solid Waste Research, Tehran University of Medical Sciences, Tehran, Iran. ³Department of Chemical Engineering, Faculty of Engineering, Razi University, Kermanshah, Iran. ⁴Department of Environment Health Engineering, School of Health, Infectious Diseases Research Center, Gonabad University of Medical Sciences, Gonabad, Iran. ⁵PhD Student of Environment Health Engineering, Student Workgroup of Social Development and Health Promotion Research Center, Gonabad University of Medical Sciences, Gonabad, Iran. ⁶Social Determinants of Health Research Center, Mashhad University of Medical Sciences, Mashhad, Iran. ✉email: shamsmh@mums.ac.ir

Of the physical, chemical, and biological technologies that exist to abate heavy metals and other contaminants, adsorption is known as a promising option due to the simplicity of design, ease of operation, and efficient removal of the contaminants in trace levels^{20,21}. The process is especially viable when it is accomplished with available and low-cost adsorbents. Seeking cheap, natural, abundant, and environmentally friendly adsorbents for heavy metals was being an interest in different studies^{22–26}. Low-cost zeolite²⁷, Eupatorium Adenophorum spreng²⁸, dry desulfurization slag²⁹, manganoxide³⁰, reed root, sawdust, seaweed³¹, fly ash^{32,33}, and nopal cladodes³⁴, were successfully employed against Pb(II) in a lab or full-scale treatment units. Moreover, Lingamdinne et al. used *Lonicera japonica* flower powder and the magnetized form as low-cost, eco-friendly, and efficient adsorbents against Co(II), Pb(II), and Co(II)^{35,36}.

Valorization of waste materials and byproducts into a useful adsorbent is a promising option to prevent waste generation and to have an economic adsorption system³⁷. In this context, the use of pottery wastes produced in a huge amount during the production and transportation of ceramic industries would have environmental and economic advantages.

Pottery waste produced in different countries has been studied for environmental remediation and as a structural material³⁸. Bouatay et al. valorized Tunisian Pottery Clay as a low-cost material for Basic dyes and realized the adsorption capacity was in the range of commercial powdered activated carbon³⁹. Hao et al. prepared a carbon/pottery composite for fluoride uptake and demonstrated a good adsorption efficacy of 88.56% and an adsorption capacity of 2.214 mg/g⁴⁰. Khazali et al. highlighted the presence of large deposits of clay minerals in different locations in Jordan and studied the possibility of Jordanian pottery materials for copper(II) adsorption⁴¹.

Herein, the pottery granules (PG) which are environmentally benign, low cost and abundant waste material, were studied against Pb(II) in the aqueous medium. After minimal preparation steps, PG was characterized and used in a batch sorption system to evaluate the effect of key operating variables i.e. pH, adsorbent dose, and the presence of competitive ions, on Pb(II) adsorption. The non-linear kinetic and equilibrium models fitted the experiments to elucidate the mechanisms that govern the adsorption. Moreover, the economic viability of the adsorption to scale up to the real treatment system is justified.

Material and methods

Adsorbent preparation and characterization. Except for pottery granules (PG), all the chemicals used in the study were of analytical grade and obtained from Merck. Pb(II) solutions with desired concentration prepared from a 100 mg/L stock solution prepared by Pb(NO₃)₂. Pottery wastes were obtained from the local pottery manufactories, washed thoroughly with deionized water, and oven-dried at 70 °C for 24 h. Pottery wastes were then crushed in a ball mill, and sieved with a stainless steel #20 (0.84 mm) screener to obtain a uniform granular particle size. The structural characteristics of PG were analyzed by x-ray diffraction (XRD) and scanning electron microscope (FESEM) analysis.

The pH at zero point of charge (pH_{Zpc}) of PG was determined to determine the mechanism of Pb(II) adsorption. 0.1 g of PG was added to the solutions with initial pH in the range of 2–10 (pHi). After mixing for 24 h, the final pH was measured as pH_f. The pH_{Zpc} was then estimated from the intercept of ΔpH (pHi–pH_f) vs pHi. The pH_{Zpc} of PG was determined to be ~8.7.

Adsorption experiments. Adsorption experiments were carried out in an incubator shaker at 250 rpm at 23 ± 1 °C. Similar to temperature, pH was not controlled during the experiments and was ~5.6. Samples were taken at predetermined time intervals for Pb(II) measurement using a furnace atomic absorption spectroscopy (Varian AA240FS). The responses for the process, Pb(II) removal efficiency (Re, %), and PG adsorption capacity (q, mg/g) were calculated from Eqs. (1) and (2), respectively.

$$Re = \frac{(C_0 - C_t)}{C_0} \times 100 \quad (1)$$

$$q = \frac{(C_0 - C_t)(V)}{m} \times 100 \quad (2)$$

where C₀ and C_t (mg/L) are the concentration of Pb(II) at time = 0, and any time, V (L) is the solution volume, and m (g) is the mass of PG. To obtain the PG capacity at the equilibrium, Eq. (2) was used where q and C_t were named q_e and C_e, respectively.

The coefficient of determination (R²), Adjusted R-square (R²_{adj}), and the sum of squares error (SSE) are useful statistical parameters to determine the suitability and accuracy of the models. As R² value is close to unity, the model describes the data more accurately. This is also the case for R²_{adj}, however, R²_{adj} value does not always get close to unity by the number of inputted variables. Another parameter, the sum of square error (SSE), reveals the difference between data for the experiments and their corresponding values estimated by the model. The model with a lower SSE would have a more precise estimation.

Nonlinear regression models were applied to the experimental data for kinetic and equilibrium studies. Compared to linear forms, nonlinear regression provides a more precise estimation of the model terms. Nonlinear models for isotherm and kinetic studies and the statistical parameters used for the suitability of the models are summarized in Table 1.

Type of equation	Nonlinear form	Parameters
Isotherm models		
Langmuir	$q_e = \frac{Q_m K_L C_e}{1 + K_L C_e}$	C_e = adsorbate equilibrium concentration (mg/L) q_e = adsorption capacity at equilibrium (mg/g) Q_m = monolayer coverage capacity (mg/g) K_L = Langmuir isotherm constant (L/mg)
Freundlich	$q_e = K_f C_e^{1/n}$	K_f = Freundlich isotherm constant (mg ^{1-(1/n)} L ^{1/n} g ⁻¹) n = adsorption intensity
Sips	$q_e = \frac{q_{ms} K_s C_e^{m_s}}{1 + K_s C_e^{m_s}}$	q_{ms} = Sips maximum adsorption capacity (mg/g) K_s = Sips equilibrium constant (L/mg) ^{m_s} m_s = Sips model exponent
Hill	$q_e = \frac{qH C_e^{nH}}{K_D + C_e^{nH}}$	qH = Maximum uptake saturation (mg/L) C_e^{nH} , K_D = Hill constants
Redlich-Peterson	$q_e = \frac{K_{RP} C_e}{1 + a_{RP} C_e^g}$	K_{RP} = Redlich-Peterson isotherm constant (L/g) a_{RP} = Redlich-Peterson model constant (mg/L) ^g g = Redlich-Peterson model exponent
Khan	$q_e = \frac{q_b b_k}{(1 + b_k C_e)^{aK}}$	bK = is the Khan model constant aK = Khan model exponent
Kinetic models		
Pseudo first-order	$\frac{dq_t}{dt} = k_1 (q_e - q_t)$	q_e = adsorption capacity at equilibrium (mg/g) q_t = adsorption capacity at any time (mg/g) k_1 = Rate constant min ⁻¹
Pseudo second-order	$\frac{dq_t}{dt} = k_2 (q_e - q_t)^2$	k_2 = Rate constant (g/(mg min))
Intraparticle diffusion kinetic	$q_t = K_t \times t^{0.5} + C_t$	K_t = Rate constant (mg/(g min))
Statistical parameter		
Coefficient of determination (R ²)	$R^2 = 1 - \frac{\sum_{i=1}^n (y_{ip} - y_i)^2}{\sum_{i=1}^n (y_{ip} - \bar{y})^2}$	y_{ip} = The predicted value by the model y_i = The observed value
Adjusted R-square (R ² adj)	$R^2_{adj} = 1 - \left(\frac{n-1}{1-(n_p+1)} \right) (1 - R^2)$	\bar{y} = Mean of observed value n_p = The number of variables in the model
Sum of squares error (SSE)	$SSE = \sum_{i=1}^n (y_{ip} - y_i)^2$	

Table 1. The models and statistical parameters used in this study 42,43.

Results and discussion

Adsorbent characteristics. Figure 1 shows the FESEM images of PG with two magnifications. As seen, PG is composed of aggregations of amorphous particles. Moreover, the presence of frequent voids and pores in the figures reflected the porous nature of the structure. The structural composition and crystalline phases of PG were also determined by XRD and the results are presented in Fig. 2. As seen, the chemical composition of PG mainly composed of Al₂ Ca O₁₂ Si₄ (52%), C₂ Ca Mg O₆ (31.4%), and SiO₂ (16.2%).

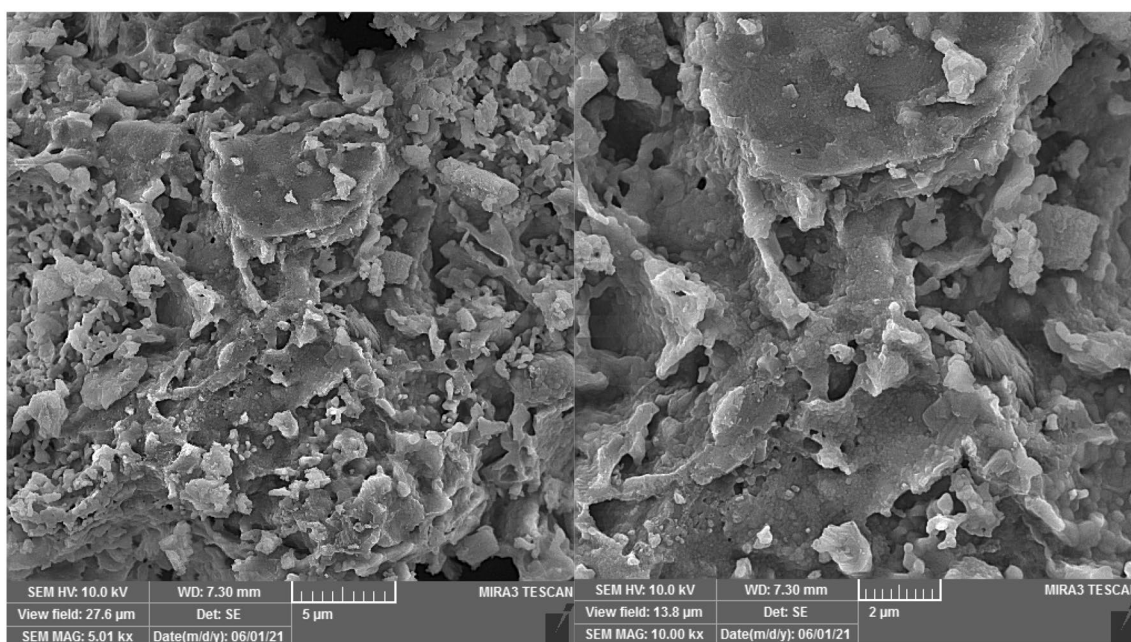


Figure 1. FESEM of PG adsorbent with two magnification.

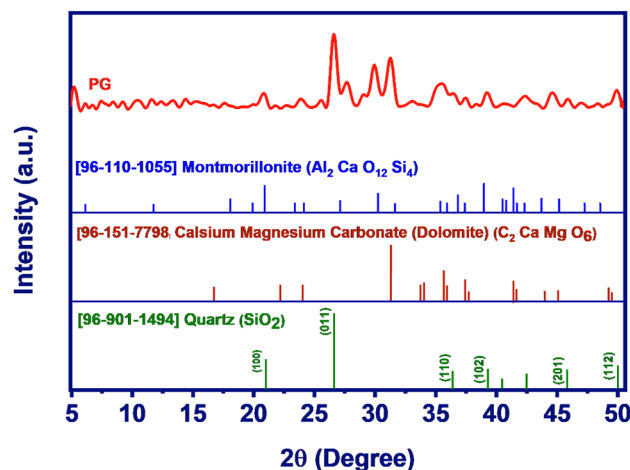


Figure 2. XRD pattern of PG used for Pb(II) removal.

Effect of PG dose, mixing time, and Pb(II) concentration. Contact time and adsorbent dose are important variables that determine the economic viability of the process in real treatment plants. Pb(II) removal was determined as a function of PG masses added to the solutions. As shown in Fig. 3, Pb(II) adsorption increased significantly by dose from 5 to 15 g/L. Similar findings were observed for antibiotics⁴⁴ and Pb(II)⁴⁵ attributed to the frequently available sorption sites for contaminants under elevated doses. The figure also shows that the removal was not changed significantly when the adsorbent dose increased by 10 g/L. Pb(II) uptake is also dependent on the mixing time for all adsorbent doses. For instance, a sharp increase in adsorption of Pb(II) from about 35% to ~93% was observed in Fig. 3 by time in the range of 5–60 min. It can also be deduced from the figure that the PG rapidly uptake Pb(II) and the equilibrium was almost reached within 30 min. The fast adsorption is of economic and operational advantages, as the treatment unit could operate in small size and high rate mode.

Figure 4 plotted the removal efficiency of PG for Pb(II) under the different initial concentrations. The figure clearly showed a declining in Pb(II) adsorption by increasing the metal concentration. This behavior could be explained by the higher competition developed for Pb(II) ions to adsorb on limited sorption sites that exist on the surface. The adsorbent capacity (q_t) for Pb(II), on the other hand, increased significantly by increasing Pb(II) ions in the solution. As indicated in Fig. 5, increasing adsorbent capacity by Pb(II) concentration reflected an efficient utilization of adsorbent sites.

Effect of pH. pH is known as a key physicochemical variable that controls the adsorption process by directing the electrostatic interactions by changing the ionic state of the chemicals in water and also the adsorbent surface charge⁴³. The effect of solution pH was studied in the range of 2–12. As presented in Fig. 6, Pb(II) adsorption was favorable at alkaline conditions and Pb(II) removal decreased from ~97 to ~45% when pH decreased

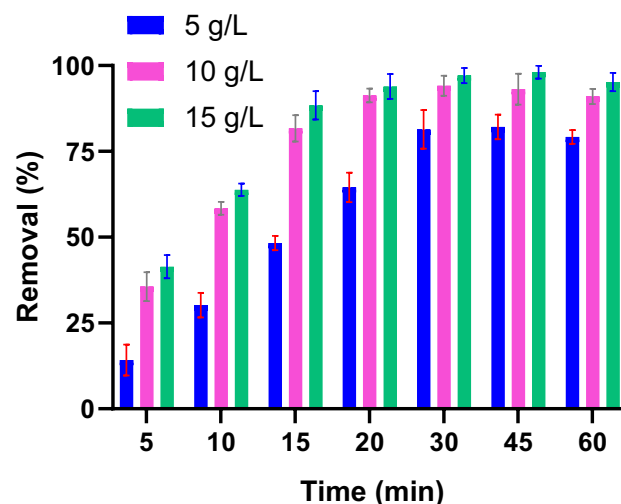


Figure 3. Pb(II) removal as a function of adsorbent dose (Pb(II): 10 mg/L).

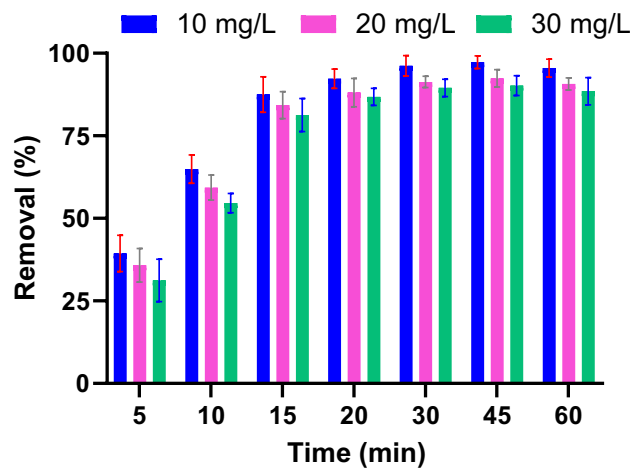


Figure 4. Pb(II) removal as a function of Pb(II) concentrations. (PG: 10 g/L).

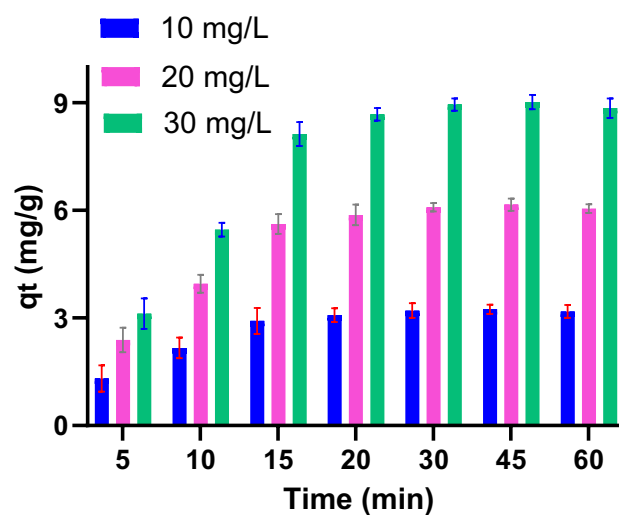


Figure 5. Adsorbent capacity (qt) as a function of Pb(II) concentration (PG: 10 g/L).

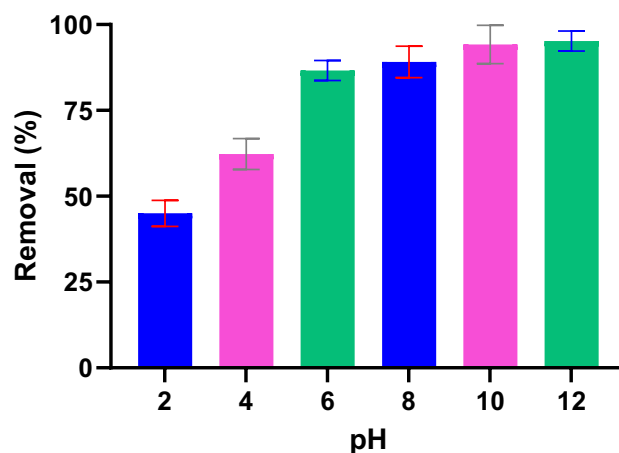


Figure 6. Effect of pH on Pb(II) adsorption (PG: 10 g/L, Pb(II): 10 mg/L).

from 12 to 2. Low pH was not favored Pb(II) adsorption, however, the removal rate remained above 60% at pH 4. The mechanism of Pb(II) adsorption as a function of pH could explain by the ionic species of Pb(II) and PG surface charge. The pH_{ZPC} of PG was determined to be ~ 8.7 that means at $\text{pH} < 8.7$ the surface of PG is positively charged. Under the strong acidic condition, the H_3O^+ and Pb^{2+} species dominated in the solution, and a net repulsive force developed between these cations and PG⁺ surface. Studies on clay⁴⁶ and granulated blast-furnace slag⁴⁷ also showed that Pb(II) removal depends strongly on the pH of solutions and removal dropped dramatically as pH decreased.

Effect of temperature. Study the solution temperature in sorption systems is essential since it is a common phenomenon in real water treatment systems. To realize how solution temperature affects Pb(II) removal, experiments were carried out at temperatures ranging from 15 to 45 °C. As seen in Fig. 7, Pb(II) adsorption increases by 18% when the temperature raised in the studied range.

An improved adsorption performance of Pb(II) onto PG by increasing the solution temperature is indicative of the endothermic nature of the process. Adsorption of Pb(II) ions as a function of temperature was studied for different adsorbents in the literature. Hefne et al. studied the Pb(II) adsorption onto natural bentonite in the range of 293–313 K and found the process is endothermic and spontaneous⁴⁸. Wan Ngah et al. studied the Pb(II) and Cu(II) removal by natural composite chitosan-tripolyphosphate beads and realized the adsorption of both metals are endothermic⁴⁹. Pb(II) adsorption onto Turkish kaolinite clay as a natural and abundant mineral studied by Sari et al. and found to be exothermic⁵⁰.

Kinetic study. Kinetic and Isotherm models could give essential parameters for the design and operation of adsorption systems. The capacity of an adsorbent for a specific contaminant and the rate of sorption were addressed in equilibrium and kinetic modeling, respectively. To model the kinetics of Pb(II) adsorption, the removal efficiency was monitored as a function of mixing time and initial metal concentration (10, 20, and 30 mg/L). The nonlinear forms of pseudo-first-order, pseudo-second-order, and intraparticle diffusion (Weber-Morris) models described in Table 1 were used to figure out the best kinetic model^{20,51}. The graphical representation of kinetic modeling is presented in Fig. 8. Kinetic and statistical parameters are summarized in Table 2. As seen in the table, the pseudo-first-order model has a higher R^2 and R_{Adj}^2 and smaller RSS that indicate the suitability of this model to describe the kinetic data.

Equilibrium study. As discussed earlier, equilibrium studies are important in the economy of sorption because it determines the mass of adsorbent required to treat contaminated stream⁵². The data from equilibrium experiments were fitted to the most frequently used models. The Langmuir, Freundlich, Sips, Redlich-Peterson, Hill, and Khan isotherm models as listed in Table 1 fitted to equilibrium data and the results presented in Fig. 9. Also, Table 3 summarized the isotherm parameters for Pb(II) adsorption by PG. As seen, R^2 and R_{adj}^2 are closest to unity and RSS in minimum for the Freundlich model. The Freundlich equation is an empirical equation that described the adsorption to occur as multilayers onto a heterogeneous surface. This finding endorsed the porous structure of PG as discussed in the characterization section.

K_F is a constant relating to the affinity of the adsorbate to the adsorbent. A large value of K_F in the Freundlich model implies the high affinity of Pb(II) for PG. Furthermore, $1/n$ value less than unity indicates the adsorption process is favorable.

Q_{max} in Langmuir isotherm indicates the monolayer adsorption capacity of PG and is a useful tool to compare different adsorbents for a specific contaminant. Table 4 shows the monolayer adsorption capacity of 9.47 mg/g in the present study was in the range or higher than many of those for low-cost adsorbents in the literature.

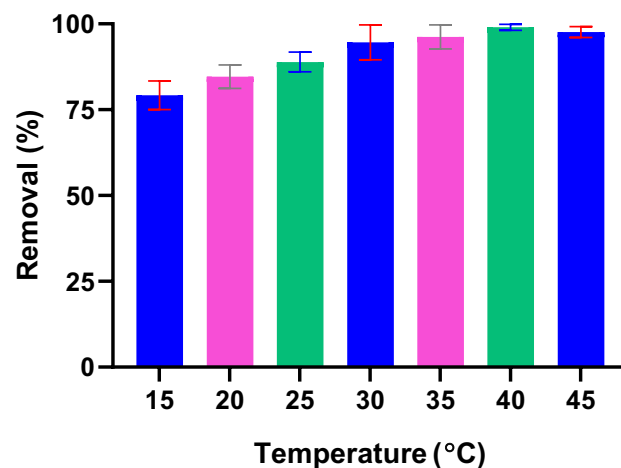


Figure 7. Effect of temperature on Pb(II) adsorption (PG: 10 g/L, Pb(II): 10 mg/L).

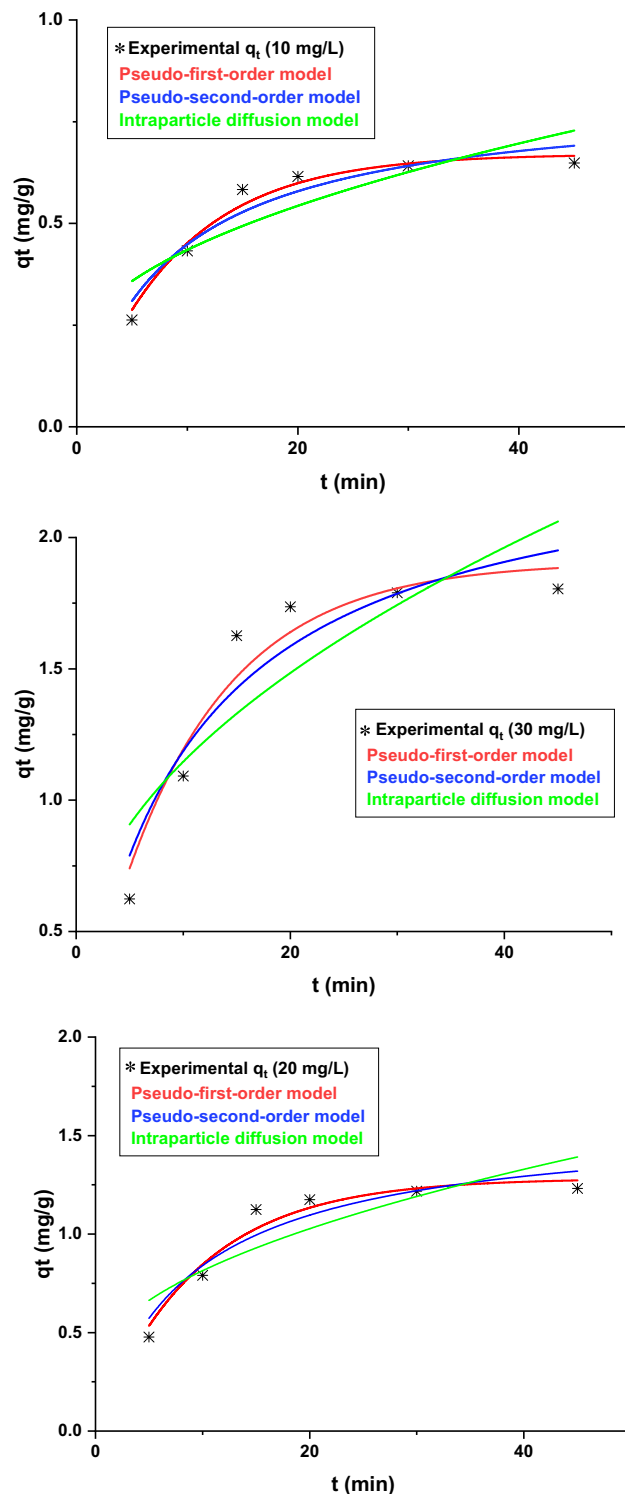


Figure 8. Fitting the three widely kinetic models for Pb(II) adsorption by Pb(II).

Effect of interfering ions. Natural waters always have a complex matrix of organic and inorganic impurities that affects the adsorbent-adsorbate interactions. The performance of the adsorption system needs to evaluate in the presence of major co-existing ions. Figure 10 illustrated how co-existing ions at the concentrations that are normally found in the water matrix affect Pb(II) adsorption. As seen, the level of inhibition by cationic ions decreased by manganese > iron > zinc > cadmium > magnesium > sodium. Furthermore, as the figure shows, increasing the ionic strength of any particular cation slightly affects the Pb(II) removal.

Concentration (mg/L)	10	20	30
q_e , exp (mg/g)	0.64	1.23	1.80
Pseudo-first order model			
q_e (mg/g)	0.67	1.28	1.9
k_1 (min^{-1})	0.11	0.1	0.11
R^2_{Adj}	0.96	0.95	0.93
R^2	0.97	0.94	0.94
RSS	0.00	0.02	0.06
Pseudo-second order model			
q_e (mg/g)	0.81	1.57	2.39
k_2 (g/mg min)	0.14	0.07	0.04
R^2_{Adj}	0.90	0.88	0.87
R^2	0.92	0.90	0.89
RSS	0.00	0.04	0.12
Interparticle diffusion model			
k_3	0.08	0.16	0.25
C	0.17	0.29	0.33
R^2_{Adj}	0.69	0.67	0.67
R^2	0.75	0.73	0.73
RSS	0.03	0.12	0.30

Table 2. Kinetic parameters for Pb(II) adsorption by PG.

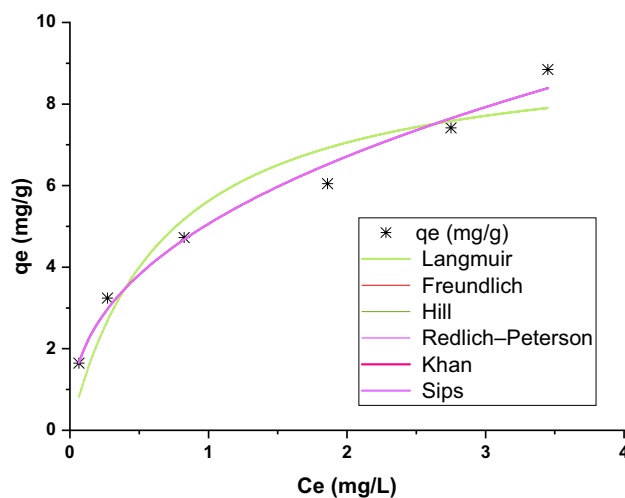


Figure 9. Fitting the six widely isotherm models for Pb(II) adsorption by Pb(II).

PG adsorption cost. The cost of the adsorption system is a critical factor that determines the feasibility of the process, particularly in remote areas and low-income countries. One strategy to minimize the cost of the adsorption system is the use of waste materials or byproducts without or by minimal preparation steps. In particular, this approach led to the production of fewer waste streams and subsequent environmental and economic issues. Industries are increasingly under pressure to manage their wastes and valorization of the waste materials is also an interest from an industry viewpoint. The comparative cost analysis for low-cost and engineered adsorbents is not simply possible as it is rarely discussed in the literature. Previous reports classified adsorbents based on the origin, and the number of modification steps they required. A material could categorize as low-cost if the cost of preparation is lower than 1 \$ per Kg⁶⁰. PG used in this study was a cheap material obtained from the local pottery manufactories. The possibility of the use of a large amount of waste produced by pottery industries, and the absence of any chemical/thermal treatment, listed PG among the low-cost adsorbents.

Conclusion

Present work reports the valorization of PG as a cheap, available, environmentally benign, and efficient sorbent for toxic Pb(II). Sorption experiments were conducted to determine how the physicochemical properties of the sorption system influence the Pb(II) adsorption. Fast adsorption and equilibrium time of about 30 min

Isotherm	Parameters	Values
Langmuir	b ($L\ mg^{-1}$)	1.46
	Q_{max} (mg/g)	9.47
	R^2_{Adj}	0.89
	R^2	0.91
	RSS	2.89
Freundlich	K_f ($mg\ g^{-1}$) (mg^{-1}) ^{1/n}	5.06
	n	2.45
	R^2_{Adj}	0.98
	R^2	0.98
	RSS	0.56
Sips	q_{ms} ($mg\ g^{-1}$)	1564.64
	K_s ($L\ mg^{-1}$) ^{ms}	0.003
	m_s	0.40
	R^2_{Adj}	0.97
	R^2	0.98
	RSS	0.57
Hill	qH	185,675.49
	K_D	36,684.36
	nH	0.40
	R^2_{Adj}	0.97
	R^2	0.98
	RSS	0.57
Redlich-Peterson	k_{RP} ($L\ g^{-1}$)	305,231.43
	a_{RP} ($mg\ L^{-1}$) ^{-bRP}	60,301.59
	b_{RP}	0.59
	R^2_{Adj}	0.97
	R^2	0.98
	RSS	0.56
Khan	q_s ($mg\ g^{-1}$)	0.14
	b_K	6244.36
	a_K	0.59
	R^2_{Adj}	0.97
	R^2	0.98
	RSS	0.57

Table 3. Nonlinear equilibrium model parameters for Pb(II) adsorption.

Adsorbent	Q_{max} (mg/g)	References	Adsorbent	Q_{max} (mg/g)	References
Active carbon	6.68	53	Diatomaceous earth	8.5	54
Kaolin	4.50		Sporopollenin	8.5	55
Bentonite	7.56		Acacia nilotica	2.51	56
Blast furnace slag	5.52		Pinus pinaster bark	1.59–3.33	57
Fly ash	4.98		Tobacco stems	5.5–5.7	58
Perlite	8.906	59	Pottery granules	9.47	Present study

Table 4. Comparison of monolayer adsorption capacity for Pb(II) by different low-cost adsorbents.

reflect the suitability of PG in real treatment systems. A higher adsorption efficiency by PG doses and mixing time observed is the result of more chance for Pb(II) to uptake by sorption sites. Alkaline pH and elevated solution temperature favored the adsorption process. Kinetic studies showed that the first-order kinetic model better describes the sorption process. Moreover, higher correlation factors for the Freundlich isotherm model, demonstrate multilayer adsorption of Pb(II) onto the heterogeneous surface of PG. The Freundlich constants also revealed the favorable nature of Pb(II) adsorption onto PG. Based on the nonlinear Langmuir model, the maximum monolayer adsorption capacity of PG was estimated to be 9.47 mg Pb(II)/g. The study of competitive

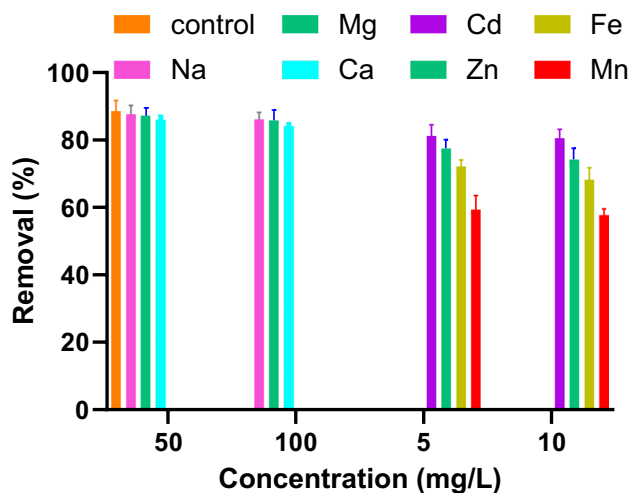


Figure 10. Effect of co-existing ions on Pb(II) adsorption by PG (adsorbent dosage: 10 g/L, Pb(II): 10 mg/L).

co-current ions showed that the adsorption of Pb(II) was hindered significantly in the presence of Mn and followed in the order of Fe > Zn > Cd > Ca > Mg > Na.

Data availability

The datasets used and/or analyzed during the current study are available from the corresponding author on reasonable request.

Received: 30 November 2022; Accepted: 8 February 2023

Published online: 25 February 2023

References

- Sani, A., Idris, K. M., Abdullahi, B. A. & Darma, A. I. Bioaccumulation and health risks of some heavy metals in *Oreochromis niloticus*, sediment and water of Challawa river, Kano, Northwestern Nigeria. *Environ. Adv.* **7**, 100172. <https://doi.org/10.1016/j.envadv.2022.100172> (2022).
- Mohammadi, A. A., Yousefi, M., Soltani, J., Ahangar, A. G. & Javan, S. Using the combined model of gamma test and neuro-fuzzy system for modeling and estimating lead bonds in reservoir sediments. *Environ. Sci. Pollut. Res.* **25**, 30315–30324 (2018).
- Narasimharao, K. *et al.* Synthesis and characterization of hexagonal MgFe layered double hydroxide/graphene oxide nanocomposite for efficient adsorptive removal of cadmium ion from aqueous solutions: Isotherm, kinetic, thermodynamic and mechanism. *J. Water Process Eng.* **47**, 102746. <https://doi.org/10.1016/j.jwpe.2022.102746> (2022).
- El-Arish, N., Zaki, R. M., Miskan, S., Setiabudi, H. & Jaafar, N. Adsorption of Pb (II) from aqueous solution using alkaline-treated natural zeolite: Process optimization analysis. *Total Environ. Res. Themes* **3**, 100015 (2022).
- Dehghani, M. & Fadaei, A. Potocatalytic oxidation of organophosphorus pesticides using zinc oxide. *Res. J. Chem. Environ.* **16**. <https://doi.org/10.1039/D0RA01741H> (2012).
- Agarwal, S. *et al.* Degradation of azinphos-methyl and chlorpyrifos from aqueous solutions by ultrasound treatment. *J. Mol. Liq.* **221**, 1237–1242. <https://doi.org/10.1016/j.molliq.2016.04.076> (2016).
- Dehghani, M., Najafpoor, A. & Azam, K. Using sonochemical reactor for degradation of LAS from effluent of wastewater treatment plant. *Desalination* **250**, 82–86 (2010).
- Machida, M., Fotoohi, B., Amamo, Y. & Mercier, L. Cadmium(II) and lead(II) adsorption onto hetero-atom functional mesoporous silica and activated carbon. *Appl. Surf. Sci.* **258**, 7389–7394. <https://doi.org/10.1016/j.apsusc.2012.04.042> (2012).
- Fakhri, Y. *et al.* Carcinogenic and non-carcinogenic health risks of metal(oid)s in tap water from Ilam city, Iran. *Food Chem. Toxicol.* **118**, 204–211. <https://doi.org/10.1016/j.fct.2018.04.039> (2018).
- Esmailzadeh, M. *et al.* Investigation of the extent of contamination of heavy metals in agricultural soil using statistical analyses and contamination indices. *Hum. Ecol. Risk Assess. Int. J.* **25**, 1125–1136 (2019).
- Bradley, P. M. *et al.* Mixed organic and inorganic tapwater exposures and potential effects in greater Chicago area, USA. *Sci. Total Environ.* **719**, 137236 (2020).
- Chu, W. *et al.* A biomimetic sensor for the detection of lead in water. *Biosens. Bioelectron.* **67**, 621–624. <https://doi.org/10.1016/j.bios.2014.09.077> (2015).
- Wadhwa, S. K., Tuzen, M., Kazi, T. G., Soylyak, M. & Hazer, B. Polyhydroxybutyrate-b-polyethyleneglycol block copolymer for the solid phase extraction of lead and copper in water, baby foods, tea and coffee samples. *Food Chem.* **152**, 75–80. <https://doi.org/10.1016/j.foodchem.2013.11.133> (2014).
- Ngueta, G. *et al.* Exposure of young children to household water lead in the Montreal area (Canada): The potential influence of winter-to-summer changes in water lead levels on children's blood lead concentration. *Environ. Int.* **73**, 57–65. <https://doi.org/10.1016/j.envint.2014.07.005> (2014).
- Shokri, S. *et al.* Risk assessment of heavy metals consumption through onion on human health in Iran. *Food Chem. X* **14**, 100283 (2022).
- Ritter, K. S. *et al.* Sources, pathways, and relative risks of contaminants in surface water and groundwater: A perspective prepared for the Walkerton inquiry. *J. Toxicol. Environ. Health Part A* **65**, 1–142 (2002).
- Peiravi, R., Alidadi, H., Dehghan, A. A. & Vahedian, M. Heavy metals concentrations in Mashhad drinking water network. *Zahedan J. Res. Med. Sci.* **15**, 74–76 (2013).

18. Roy, S. & Edwards, M. A. Preventing another lead (Pb) in drinking water crisis: Lessons from the Washington DC and Flint MI contamination events. *Curr. Opin. Environ. Sci. Health* **7**, 34–44 (2019).
19. Edzwald, J. *Water Quality & Treatment: A Handbook on Drinking Water* (McGraw-Hill Education, 2011).
20. Yousefi, M. *et al.* Comparison of LSSVM and RSM in simulating the removal of ciprofloxacin from aqueous solutions using magnetization of functionalized multi-walled carbon nanotubes: Process optimization using GA and RSM techniques. *J. Environ. Chem. Eng.* **9**, 105677. <https://doi.org/10.1016/j.jece.2021.105677> (2021).
21. Mohammadi, A. A., Dehghani, M. H., Mesdaghinia, A., Yaghmaian, K. & Es'haghi, Z. Adsorptive removal of endocrine disrupting compounds from aqueous solutions using magnetic multi-wall carbon nanotubes modified with chitosan biopolymer based on response surface methodology: Functionalization, kinetics, and isotherms studies. *Int. J. Biol. Macromol.* **155**, 1019–1029. <https://doi.org/10.1016/j.ijbiomac.2019.11.065> (2020).
22. Wang, P. *et al.* Structure regulation of silica nanotubes and their adsorption behaviors for heavy metal ions: pH effect, kinetics, isotherms and mechanism. *J. Hazard. Mater.* **286**, 533–544. <https://doi.org/10.1016/j.jhazmat.2014.12.034> (2015).
23. Mahmoud Shams, M. Q., Sina, D. & Amir, H. M. Evaluation of waste aluminum filing in removal of fluoride from aqueous solution. *Fresenius Environ. Bull.* **22**, 6 (2013).
24. Mahmoud Shams, I. N., Sina, D., Bahman, R., Mehdi, Q. & Mojtaba, A. An environmental friendly and cheap adsorbent (municipal solid waste compost ASH) with high efficiency in removal of phosphorus from aqueous solution. *Fresenius Environ. Bull.* **22**, 5 (2013).
25. Koduru, J. R. *et al.* *Rare-Earth Metal Recovery for Green Technologies* 87–109 (Springer, 2020).
26. Qasemi, M. *et al.* Thermally treated aluminium waste-filings, a low cost and efficient adsorbent for phosphorus removal from water. *Global NEST J.* **20**, 488–496 (2018).
27. Salem, A. & Akbari Sene, R. Removal of lead from solution by combination of natural zeolite-kaolin-bentonite as a new low-cost adsorbent. *Chem. Eng. J.* **174**, 619–628. <https://doi.org/10.1016/j.cej.2011.09.075> (2011).
28. Guo, S. *et al.* Kinetics and equilibrium adsorption study of lead(II) onto the low cost adsorbent^o Eupatorium adenophorum spreng. *Process Saf. Environ. Prot.* **87**, 343–351. <https://doi.org/10.1016/j.psep.2009.06.003> (2009).
29. Wu, Q., You, R., Clark, M. & Yu, Y. Pb(II) removal from aqueous solution by a low-cost adsorbent dry desulfurization slag. *Appl. Surf. Sci.* **314**, 129–137. <https://doi.org/10.1016/j.apsusc.2014.06.154> (2014).
30. Sonmezay, A., Oncel, M. S. & Bektas, N. Adsorption of lead and cadmium ions from aqueous solutions using manganese minerals. *Trans. Nonferrous Met. Soc. China* **22**, 3131–3139. [https://doi.org/10.1016/S1003-6326\(12\)61765-8](https://doi.org/10.1016/S1003-6326(12)61765-8) (2012).
31. Akunwa, N. K., Muhammad, M. N. & Akunna, J. C. Treatment of metal-contaminated wastewater: A comparison of low-cost biosorbents. *J. Environ. Manag.* **146**, 517–523. <https://doi.org/10.1016/j.jenvman.2014.08.014> (2014).
32. Angaru, G. K. R., Lingamdinne, L. P., Koduru, J. R. & Chang, Y.-Y. N-cetyltrimethylammonium bromide-modified zeolite Na-A from waste fly ash for hexavalent chromium removal from industrial effluent. *J. Compos. Sci.* **6**, 256 (2022).
33. Angaru, G. K. R. *et al.* Encapsulated zerovalent iron/nickel-fly ash zeolite foam for treating industrial wastewater contaminated by heavy metals. *Mater. Today Chem.* **22**, 100577. <https://doi.org/10.1016/j.mtchem.2021.100577> (2021).
34. Miretzky, P., Munoz, C. & Carrillo-Chávez, A. Experimental binding of lead to a low cost on biosorbent: Nopal (*Opuntia streptacantha*). *Bioresour. Technol.* **99**, 1211–1217. <https://doi.org/10.1016/j.biortech.2007.02.045> (2008).
35. Lingamdinne, L. P., Yang, J.-K., Chang, Y.-Y. & Koduru, J. R. Low-cost magnetized *Lonicera japonica* flower biomass for the sorption removal of heavy metals. *Hydrometallurgy* **165**, 81–89. <https://doi.org/10.1016/j.hydromet.2015.10.022> (2016).
36. Lingamdinne, L. P., Koduru, J. R., Jyothi, R. K., Chang, Y.-Y. & Yang, J.-K. Factors affect on bioremediation of Co (II) and Pb (II) onto *Lonicera japonica* flowers powder. *Desalin. Water Treat.* **57**, 13066–13080 (2016).
37. Narasimharao, K. *et al.* Orange waste Biochar-Magnesium Silicate (OBMS) composite for enhanced removal of U(VI) ions from aqueous solutions. *J. Water Process Eng.* **51**, 103359. <https://doi.org/10.1016/j.jwpe.2022.103359> (2023).
38. Ulubeyli, G. Ç., Bilir, T. & Artir, R. Ceramic wastes usage as alternative aggregate in mortar and concrete. *Period. Eng. Nat. Sci. (PEN)* **5**. <https://doi.org/10.21533/pen.v5i2.115> (2017).
39. Bouatay, F., Dridi, S. & Mhenni, M. Valorization of tunisian pottery clay onto basic dyes adsorption. *Int. J. Environ. Res.* **8**. <https://doi.org/10.22059/ijer.2014.799> (2014).
40. Jin, H. *et al.* Research on carbon/pottery adsorption composite for removing fluoride. *Sci. Silvae Sin.* **47**, 147–151 (2011).
41. Khazali, O., Abu-El-Halawa, R. & Al-Sou'od, K. Removal of copper (II) from aqueous solution by Jordanian pottery materials. *J. Hazardous Mater.* **139**, 67–71 (2007).
42. Talebi, S. S. *et al.* Defluoridation of drinking water by metal impregnated multi-layer green graphene fabricated from trees pruning waste. *Environ. Sci. Pollut. Res.* **28**, 18201–18215 (2021).
43. Lingamdinne, L. P., Lebaka, V. R., Koduru, J. R. & Chang, Y.-Y. Insights into manganese ferrite anchored graphene oxide to remove Cd(II) and U(VI) via batch and semi-batch columns and its potential antibacterial applications. *Chemosphere* **310**, 136888. <https://doi.org/10.1016/j.chemosphere.2022.136888> (2023).
44. Shams, M. *et al.* Parameter optimization of tetracycline removal by vanadium oxide nano cuboids. *Colloids Surf. A Physicochem. Eng. Asp.* **619**, 126460. <https://doi.org/10.1016/j.colsurfa.2021.126460> (2021).
45. Khan, M., Hegde, R. & Shabiimam, M. Adsorption of lead by bentonite clay. *Int. J. Sci. Res. Manag.* **5**, 5800–5804 (2017).
46. Al-Jlil, S. A. & Alsewailam, F. D. Saudi Arabian clays for lead removal in wastewater. *Appl. Clay Sci.* **42**, 671–674 (2009).
47. Dimitrova, S. V. & Mehandgiev, D. R. Lead removal from aqueous solutions by granulated blast-furnace slag. *Water Res.* **32**, 3289–3292. [https://doi.org/10.1016/S0043-1354\(98\)00119-5](https://doi.org/10.1016/S0043-1354(98)00119-5) (1998).
48. Hefne, J., Mekhemer, W., Alandis, N., Aldayel, O. & Alajyan, T. Kinetic and thermodynamic study of the adsorption of Pb (II) from aqueous solution to the natural and treated bentonite. *Int. J. Phys. Sci.* **3**, 281–288 (2008).
49. Ngah, W. S. W. & Fatinathan, S. Adsorption characterization of Pb(II) and Cu(II) ions onto chitosan-tripolyphosphate beads: Kinetic, equilibrium and thermodynamic studies. *J. Environ. Manag.* **91**, 958–969. <https://doi.org/10.1016/j.jenvman.2009.12.003> (2010).
50. Sari, A., Tuzen, M., Citak, D. & Soylak, M. Equilibrium, kinetic and thermodynamic studies of adsorption of Pb(II) from aqueous solution onto Turkish kaolinite clay. *J. Hazard. Mater.* **149**, 283–291. <https://doi.org/10.1016/j.jhazmat.2007.03.078> (2007).
51. Mohammadi, A. A. *et al.* Metal-organic framework Uio-66 for adsorption of methylene blue dye from aqueous solutions. *Int. J. Environ. Sci. Technol.* **14**, 1959–1968 (2017).
52. Deng, H. & Yu, X. Adsorption of fluoride, arsenate and phosphate in aqueous solution by cerium impregnated fibrous protein. *Chem. Eng. J.* **184**, 205–212. <https://doi.org/10.1016/j.cej.2012.01.031> (2012).
53. Mishra, P. C. & Patel, R. K. Removal of lead and zinc ions from water by low cost adsorbents. *J. Hazard. Mater.* **168**, 319–325. <https://doi.org/10.1016/j.jhazmat.2009.02.026> (2009).
54. Li, S., Li, D., Su, F., Ren, Y. & Qin, G. Uniform surface modification of diatomaceous earth with amorphous manganese oxide and its adsorption characteristics for lead ions. *Appl. Surf. Sci.* <https://doi.org/10.1016/j.apsusc.2014.08.184> (2014).
55. Unlu, N. & Ersoz, M. Adsorption characteristics of heavy metal ions onto a low cost biopolymeric sorbent from aqueous solutions. *J. Hazard. Mater.* **136**, 272–280. <https://doi.org/10.1016/j.jhazmat.2005.12.013> (2006).
56. Waseem, S., Din, M. I., Nasir, S. & Rasool, A. Evaluation of *Acacia nilotica* as a non conventional low cost biosorbent for the elimination of Pb(II) and Cd(II) ions from aqueous solutions. *Arab. J. Chem.* **7**, 1091–1098. <https://doi.org/10.1016/j.arabcj.2012.03.020> (2014).

57. Bailey, S. E., Olin, T. J., Bricka, R. M. & Adrian, D. D. A review of potentially low-cost sorbents for heavy metals. *Water Res.* **33**, 2469–2479. [https://doi.org/10.1016/S0043-1354\(98\)00475-8](https://doi.org/10.1016/S0043-1354(98)00475-8) (1999).
58. Li, W. *et al.* Tobacco stems as a low cost adsorbent for the removal of Pb(II) from wastewater: Equilibrium and kinetic studies. *Ind. Crops Prod.* **28**, 294–302. <https://doi.org/10.1016/j.indcrop.2008.03.007> (2008).
59. Irani, M., Amjadi, M. & Mousavian, M. A. Comparative study of lead sorption onto natural perlite, dolomite and diatomite. *Chem. Eng. J.* **178**, 317–323. <https://doi.org/10.1016/j.cej.2011.10.011> (2011).
60. Kumar, P. S., Korving, L., van Loosdrecht, M. C. M. & Witkamp, G.-J. Adsorption as a technology to achieve ultra-low concentrations of phosphate: Research gaps and economic analysis. *Water Res.* **X 4**, 100029. <https://doi.org/10.1016/j.wroa.2019.100029> (2019).

Acknowledgements

This research has been supported by Tehran University of Medical Sciences and by Mashhad University of Medical Science, Iran (No. 4000273).

Author contributions

M.H.D: Conceptualization, Methodology, Investigation, Formal analysis, Writing—original draft. S.A.S, M.A, M.Q: Investigation, Methodology, Writing—review & editing. M.S: Methodology, Writing—review & editing, Supervision.

Competing interests

The authors declare no competing interests.

Additional information

Correspondence and requests for materials should be addressed to M.S.

Reprints and permissions information is available at www.nature.com/reprints.

Publisher's note Springer Nature remains neutral with regard to jurisdictional claims in published maps and institutional affiliations.



Open Access This article is licensed under a Creative Commons Attribution 4.0 International License, which permits use, sharing, adaptation, distribution and reproduction in any medium or format, as long as you give appropriate credit to the original author(s) and the source, provide a link to the Creative Commons licence, and indicate if changes were made. The images or other third party material in this article are included in the article's Creative Commons licence, unless indicated otherwise in a credit line to the material. If material is not included in the article's Creative Commons licence and your intended use is not permitted by statutory regulation or exceeds the permitted use, you will need to obtain permission directly from the copyright holder. To view a copy of this licence, visit <http://creativecommons.org/licenses/by/4.0/>.

© The Author(s) 2023